Neurobiology of Disease 192 (2024) 106439

Contents lists available at ScienceDirect

Neurobiology of Disease

journal homepage: www.elsevier.com/locate/ynbdi

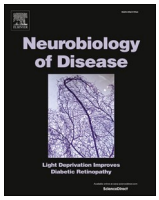

Cognitively healthy *APOE4/4* carriers show white matter impairment associated with serum NfL and amyloid-PET

Claudia Tato-Fernández [a,b,*], Laura L. Ekblad [a,b,c], Elina Pietilä [a,b], Virva Saunavaara [a,b,d], Semi Helin [b], Riitta Parkkola [e,f], Henrik Zetterberg [g,h,i,j,k,l], Kaj Blennow [g,h,m,n], Juha O. Rinne [a,b,o], Anniina Snellman [a,b]

[a] *Turku PET Centre, Turku University Hospital, Turku, Finland*
[b] *Turku PET Centre, University of Turku, Turku, Finland*
[c] *Department of Geriatric Medicine, Turku University Hospital, Turku, Finland*
[d] *Department of Medical Physics, Division of Medical Imaging, Turku University Hospital, Finland*
[e] *Department of Radiology, Turku University Hospital, Turku, Finland*
[f] *Department of Radiology, University of Turku, Turku, Finland.*
[g] *Department of Psychiatry and Neurochemistry, Institute of Neuroscience and Physiology, The Sahlgrenska Academy at the University of Gothenburg, Mölndal, Sweden*
[h] *Clinical Neurochemistry Laboratory, Sahlgrenska University Hospital, Mölndal, Sweden*
[i] *Department of Neurodegenerative Disease, UCL Institute of Neurology, Queen Square, London, UK*
[j] *UK Dementia Research Institute at UCL, London, UK*
[k] *Hong Kong Center for Neurodegenerative Diseases, Clear Water Bay, Hong Kong, China*
[l] *Wisconsin Alzheimer's Disease Research Center, University of Wisconsin School of Medicine and Public Health, University of Wisconsin-Madison, Madison, WI, USA*
[m] *Paris Brain Institute, ICM, Pitié-Salpêtrière Hospital, Sorbonne University, Paris, France*
[n] *Neurodegenerative Disorder Research Center, Division of Life Sciences and Medicine, Department of Neurology, Institute on Aging and Brain Disorders, University of Science and Technology of China and First Affiliated Hospital of USTC, Hefei, PR China*
[o] *InFLAMES Research Flagship, University of Turku, Turku, Finland*

A R T I C L E I N F O

Keywords:
Alzheimer's disease
Apolipoprotein E
APOE
Magnetic resonance imaging
MRI
Diffusion tensor imaging
DTI
Neurofilament light chain
Positron emission tomography
[^{11}C]PiB

A B S T R A C T

Except for aging, carrying the *APOE ε4* allele (*APOE4*) is the most important risk factor for sporadic Alzheimer's disease. *APOE4* carriers may have reduced capacity to recycle lipids, resulting in white matter microstructural abnormalities. In this study, we evaluated whether white matter impairment measured by diffusion tensor imaging (DTI) differs between healthy individuals with a different number of *APOE4* alleles, and whether white matter impairment associates with brain beta-amyloid (Aβ) load and serum levels of neurofilament light chain (NfL). We studied 96 participants (*APOE3/3*, $N = 37$; *APOE3/4*, $N = 39$; *APOE4/4*, $N = 20$; mean age 70.7 (SD 5.22) years, 63% females) with a brain MRI including a DTI sequence ($N = 96$), Aβ-PET ($N = 89$) and a venous blood sample for the serum NfL concentration measurement ($N = 88$). Fractional anisotropy (FA), mean diffusivity (MD), radial diffusivity (RD) and axial diffusivity (AxD) in six *a priori*-selected white matter regions-of-interest (ROIs) were compared between the groups using ANCOVA, with sex and age as covariates. A voxel-weighted average of FA, MD, RD and AxD was calculated for each subject, and correlations with Aβ-PET and NfL levels were evaluated. *APOE4/4* carriers exhibited a higher MD and a higher RD in the body of corpus callosum than *APOE3/4* ($p = 0.0053$ and $p = 0.0049$, respectively) and *APOE3/3* ($p = 0.026$ and $p = 0.042$). *APOE4/4* carriers had a higher AxD than *APOE3/4* ($p = 0.012$) and *APOE3/3* ($p = 0.040$) in the right cingulum adjacent to cingulate cortex. In the total sample, composite MD, RD and AxD positively correlated with the cortical Aβ load ($r = 0.26$ to 0.33, $p < 0.013$ for all) and with serum NfL concentrations ($r = 0.31$ to 0.36, $p < 0.0028$ for all). In conclusion, increased local diffusivity was detected in cognitively unimpaired *APOE4/4* homozygotes compared to *APOE3/4* and *APOE3/3* carriers, and increased diffusivity correlated with biomarkers of Alzheimer's disease and neurodegeneration. White matter impairment seems to be an early phenomenon in the Alzheimer's disease pathologic process in *APOE4/4* homozygotes.

* Corresponding author at: Turku PET Centre, Kiinamyllynkatu 4-8, 20521 Turku, Finland.
E-mail address: cltato@utu.fi (C. Tato-Fernández).

https://doi.org/10.1016/j.nbd.2024.106439
Received 27 October 2023; Received in revised form 9 February 2024; Accepted 13 February 2024
Available online 15 February 2024

1. Introduction

The ε4 allele for the *APOE* gene (*APOE4*) is the most important genetic risk factor for late-onset Alzheimer's disease (AD) (Corder et al., 1993). The mechanism through which *APOE4* increases the risk for AD has not yet been fully described, but the role of *APOE4* in lipid dysregulation has been recently highlighted (Blanchard et al., 2022). Apolipoprotein E (apoE) is involved in lipid transport in the brain (Espeseth et al., 2012), and lipids are essential components of the myelin sheath that encircles axons. *APOE4*-induced cholesterol dysregulations may decrease synaptogenesis and myelination (Bartzokis, 2011; Blanchard et al., 2022), which could contribute to the formation of toxic aggregates characteristic of AD, including beta-amyloid (Aβ) plaques (Lesser et al., 2011).

White matter impairment is part of the pathophysiological changes that an individual experiences over the course of AD (Bronge et al., 2002; Ingelsson et al., 2004). Diffusion tensor imaging (DTI) is a well-established magnetic resonance imaging (MRI) technique to quantify the movement of water molecules in the brain (Basser et al., 1994), which can detect early neurodegeneration in patients of AD (Palesi et al., 2018). The tensor model characterizes diffusion with six parameters: three mutually orthogonal eigenvectors and their corresponding eigenvalues (O'Donnell and Westin, 2011). Fractional anisotropy (FA), a normalized variance of the eigenvalues (Basser and Pierpaoli, 1996; O'Donnell and Westin, 2011), describes the shape of the diffusion ellipsoid at every voxel. Mean diffusivity (MD) represents total diffusion in a voxel as an average of the eigenvalues (Basser and Pierpaoli, 1996). Measures of axial (AxD) and radial (RD) diffusivity describe diffusion along the axis of maximal apparent diffusion and its two orthogonal orientations in the perpendicular plane, respectively (O'Donnell and Westin, 2011). White matter pathology often causes anisotropy to decrease, which may be concomitant with subtle changes in one, or more, of the diffusion directions (Alexander et al., 2007). DTI is sensitive to the underlying tissue microstructure; however, changes in FA, MD, RD and AxD should be interpreted with caution in healthy subjects (Jones et al., 2013).

Previous studies have consistently reported damage to white matter tracts in patients with AD (Bachman et al., 2014; Esrael et al., 2021; Gallagher et al., 2023; Lim et al., 2012; Palesi et al., 2018; Racine et al., 2014). These findings have been linked to other risk factors for AD, including the presence of at least one copy of the *APOE4* allele (Bagepally et al., 2012; Lee et al., 2016). However, studies with healthy *APOE4* carriers showed mixed results. Several DTI studies report degeneration of white matter tracts in healthy *APOE4* carriers (Bagepally et al., 2012; Cai et al., 2017; Cavedo et al., 2017; Douaud et al., 2011; Dowell et al., 2013; Gold et al., 2010; Heise et al., 2014; Nierenberg et al., 2005; Persson et al., 2006), but other investigations have been unable to replicate these findings (Adluru et al., 2014; Honea et al., 2009; Lyall et al., 2020; Nyberg and Salami, 2014; O'Dwyer et al., 2012; Westlye et al., 2012). Notably, these changes already appear in the preclinical stages of AD (Gallagher et al., 2023).

Even though previous studies have investigated the impact of *APOE* genotype on DTI metrics, the specific effects of *APOE4* homozygosity in healthy subjects are rarely analyzed. As only 25% of the Caucasian population carries the *APOE4* allele and prevalence of AD is elevated in this group (Gharbi-Meliani et al., 2021), it can be challenging to collect data from healthy elderly subjects who carry two copies of this allele. Most reports merge *APOE3/4* and *APOE4/4* when investigating the effects of *APOE4* in the brain. However, since *APOE4/4* carriers also have a higher risk of vascular factors that could affect white matter integrity, including increased LDL cholesterol levels (Lesser et al., 2011) and white matter hyperintensities (WMHs) (Lyall et al., 2020), the changes detected with DTI could be expected to be more severe.

During recent years, it has also become possible to investigate neuronal degeneration with fluid-based biomarkers; however, little is known about the association between DTI metrics and blood biomarkers of axonal degeneration in at-risk populations. Neurofilament light chain (NfL) is a protein expressed in neurons, which associates with other proteins to form the cytoskeleton of axons. Neurofilaments can be released in large quantities after axonal injury or degeneration (Schultz et al., 2020) and are nowadays measurable from easily-obtained blood samples (Gaetani et al., 2019). Elevated levels of serum NfL correlate with decreased FA and increased MD, AxD and RD, in patients of multiple sclerosis (Saraste et al., 2021) and AD (Schultz et al., 2020). To our knowledge, no previous study has investigated the relationship between serum NfL levels and DTI metrics in healthy *APOE4* carriers.

In this study, we aimed to expand previous DTI results by i) comparing the DTI metrics of healthy elderly subjects with one, two, or no copies of the *APOE4* allele and ii) exploring their association with brain Aβ load assessed by [^{11}C]PiB positron emission tomography (PET) and with serum NfL concentrations in the whole cognitively unimpaired sample. We hypothesized that *APOE4* carriers (*APOE4/4* and *APOE3/4*) would present white matter microstructural abnormalities in a gene-dose dependent way when compared to *APOE3/3* carriers. We expected that changes in tissue microstructure assessed by DTI would associate with higher levels of serum NfL and Aβ pathology measured by PET.

2. Methods

2.1. Participants

A total of one hundred and nine healthy elderly adults (mini mental-state examination [MMSE] score $\geq$ 25, CERAD total score $>$ 62 (Chandler et al., 2005), between the ages of 65 and 85 years old) from ASIC-E4 (Snellman et al., 2022) and CIRI-5Y (Ekblad et al., 2018) studies were assessed for this investigation. Data from both cohorts were acquired at Turku PET Centre. The main exclusion criteria were cognitive decline, neurological or psychiatric diseases, or contraindications for MRI and PET imaging. Participants from ASIC-E4 were recruited and *APOE* genotyped in collaboration with Auria Biobank (Turku, Finland) following a protocol already published (Snellman et al., 2022). Participants from CIRI-5Y were recruited from the Health2000 study population and *APOE* genotyped using the MassARRAY System (Sequenom, San Diego, CA) (Ekblad et al., 2018) with an adapted previously published method (Jänis et al., 2004). Both studies were approved by the Ethical Committee of the Hospital District of Southwest Finland. All participants signed a written informed consent according to the Declaration of Helsinki.

Six subjects from the initial sample could not be included because they were missing DTI data with reversed phase-encoding polarities. After examining the DTI images, two subjects (*APOE3/3*) were excluded from analysis due to enlarged CSF spaces or incomplete head coverage. There were no subjects with *APOE2/4* genotype, but five subjects had *APOE2/3* genotype. Since DTI metrics of *APOE2/3* carriers were seen to significantly differ from those of *APOE3/3*, the genotypes could not be pooled together as a non-carrier group. Furthermore, given the small sample size of *APOE2* carriers (n = 5), we lacked sufficient statistical power to reach generalizable conclusions about this group. Thus, the main analyses and results are reported with the remaining ninety-six participants (Group 1: *APOE3/3*, n = 37; Group 2: *APOE3/4*, n = 39; Group 3: *APOE4/4*, n = 20). Supplementary Table 1 and Supplementary Fig. 1 respectively show demographic and regional DTI results including *APOE2/3* carriers.

Out of the ninety-six participants who were included in the main analyses (after the exclusion of *APOE2/3* carriers), eighty-nine underwent PET imaging with the tracer [^{11}C]PiB (one participant chose not to participate in PET imaging, two participants discontinued the study, one PET scan was interrupted and three participants could not visit the site of acquisition for this session) and blood samples were acquired for eighty-eight participants (six participants could not fast before venous blood sampling and two participants discontinued the study) (Fig. 1).

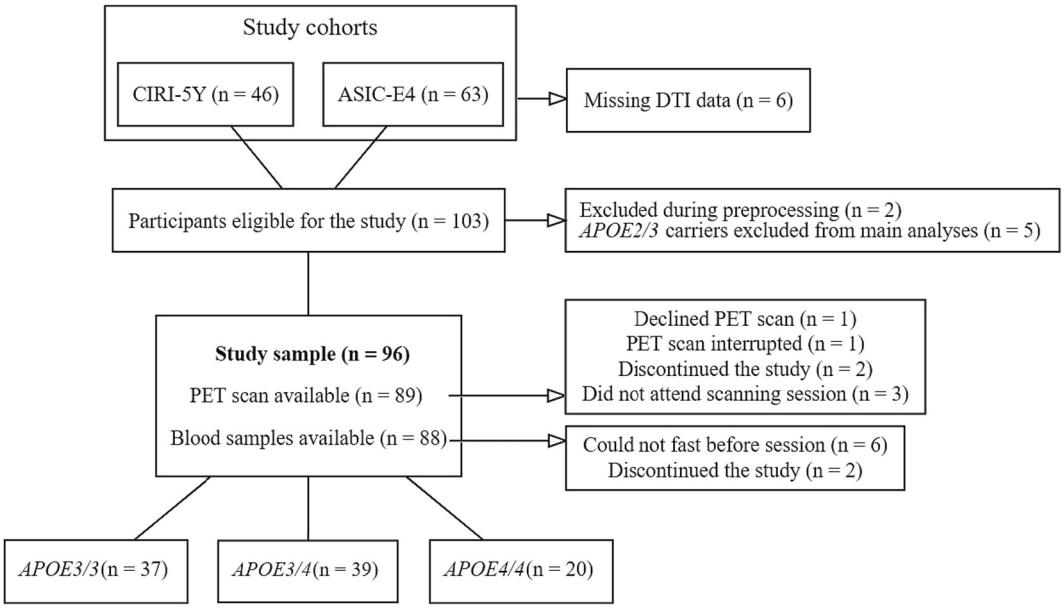

Fig. 1. Study diagram. 103 participants were eligible from two cohorts, but seven subjects were not be included in the final study. Out of the 96 participants who were analyzed, 89 underwent amyloid-PET and 88 underwent venous blood sampling.
DTI = diffusion tensor imaging, PET = positron emission tomography.

2.2. MRI acquisition

Two scanners from the same manufacturer were used during data collection due to availability at the time of acquisition. Twenty-four MRI scans were acquired with Philips Ingenia 3.0 T systems with 20-channel dS head coil (Philips Healthcare, Amsterdam, the Netherlands) and the remaining seventy-two scans were acquired with Philips Ingenuity 3.0 T TF PET-MR with 32-channel head coil (Philips Healthcare, Amsterdam, the Netherlands). In order to minimize possible confounding variation, the acquisition protocols were matched for both scanners. T1-weighted sequences, T2-weighted sequences, T2-weighted fluid-attenuated inversion recovery (FLAIR) sequences and DTI sequences were acquired for each participant. MRI images were reviewed by a neuroradiologist to exclude the presence of brain abnormalities.

The full imaging protocol has already been published (Snellman et al., 2022). DTI data were acquired using single-shot echo-planar imaging pulse sequences (TR = 6700 ms, TE = 120 ms, 2 × 2 × 2 mm voxels, 80 axial slices, slice thickness = 2 mm, no slice gap, field of view = 256 × 256 mm^2, flip angle = 90°) with sensitivity encoding (SENSE) parallel imaging. One b = 0 baseline volume was acquired with Philips Ingenia 3.0 T systems and four with Philips Ingenuity 3.0 T PET-MR, along with 63 diffusion-weighted volumes with b-values of 1000 s/mm^2. DTI sequences were followed by a single volume with b-value of 0, with the same acquisition parameters but opposing phase-encoding direction. A FLAIR image (TR = 8000 ms, TE = 337 ms, 1 × 1 × 1 mm voxels, field of view = 256 × 256 mm^2, flip angle = 90°) was used to estimate computed Fazekas score using an automatic cNeuroimage analysis tool (Combinostics Oy, Tampere, Finland), with an adapted version of methods previously described (Koikkalainen et al., 2016).

2.3. PET acquisition

PET images (n = 89) were acquired using an ECAT high-resolution research tomograph (HRRT, Siemens Medical Solutions, Knoxville, TN) with a spatial resolution of 2.5 mm. Data were acquired 40–90 min after injection of [^{11}C]PiB (dose aimed at 500 MBq, minimum 250 MBq). PET scan duration was 50 min and it was followed by a 6 min transmission scan for attenuation correction, with a ^{137}Cs point source. List-mode data was histogrammed into eight time frames (6 × 5 min; 2 × 10 min) and reconstructed with the 3D ordinary Poisson-ordered subset expectation maximization algorithm (OP-OSEM3D) with 16 subsets and 8 iterations and a voxel size of 1.22 × 1.22 × 1.22 mm.

2.4. Serum samples

Blood samples (n = 88) were acquired in the morning after a 10–12-h fasting period following in-house standard operating procedures (Snellman et al., 2022). Venous samples were analyzed at the Clinical Neurochemistry Laboratory of the University of Gothenburg (Mölndal, Sweden). The Single molecule array method and an HD-X analyzer (Quanterix) were used to measure serum NfL concentration (Simoa® NF-light™, #103186, Quanterix), following the instructions indicated by the manufacturer.

2.5. MRI processing

Image conversion from DICOM to NIFTI was done using dcm2niix v1.0.20190902 (Li et al., 2016). Manual slice-by-slice visual inspection was carried out for all volumes using FSLEyes' Lightbox to confirm the quality of image acquisition. DTI volumes were corrected for subject motion, susceptibility- and eddy-current-induced distortions using the FMRIB Software Library v6.0.1 (Smith et al., 2004). Correction for susceptibility distortion was implemented using an adapted version of the "reverse gradient method" (Andersson et al., 2003). Outlier replacement and intra-volume movement correction were applied simultaneously with eddy current correction for all subjects (Andersson et al., 2016; Andersson and Sotiropoulos, 2016). Non-brain tissue was removed using FSL's brain extraction tool (Smith, 2002). The threshold for the brain mask was individually adjusted after visual inspection. The diffusion tensor model (Basser et al., 1994) was fitted at each voxel to estimate the parameter maps for FA, MD, AxD and RD.

The ROIs were selected independently before conducting whole-brain analysis, to mitigate potential bias. The following six regions were chosen, based on previous literature researching the relationship between *APOE* gene and white matter microstructure (Adluru et al., 2014; Cai et al., 2017; Cavedo et al., 2017; Gold et al., 2010; Racine et al., 2014): uncinate fasciculus (UF), genu, body and splenium of corpus callosum (G-CC, B-CC, S-CC), cingulum bundle projections to

hippocampus (C-HC) and cingulum bundle running adjacent to the cingulate gyrus (C-CG) (Supplementary Fig. 2). UF, C-HC and C-CG were analyzed separately between hemispheres after testing that DTI metrics significantly differed with paired-sample *t*-tests.

Participants' FA, MD, AxD and RD maps were non-linearly transformed to MNI space using the FMRIB58_FA standard-space template as reference. FA maps were thresholded at 0.2 to correct for partial volume effects (PVEs). John Hopkins University (JHU) ICBM-DTI-81 atlas (Mori et al., 2008) was used to extract a brain mask of the selected ROIs. These masks were resampled to align their dimensions with the subjects' maps. Mean FA, MD, AxD and RD values were calculated by averaging the voxels within the boundaries of each ROI mask.

Whole-brain analyses were carried out within the TBSS framework (Smith et al., 2006). A mean FA image was created and skeletonized using individual FA maps projected to the FMRIB58_FA template. The tract skeleton was thresholded at a value of FA > 0.2. The non-linear warps obtained during FA image registration were subsequently applied to the MD, AxD and RD maps.

2.6. PET processing

Analysis methods of Aβ PET data and *APOE4* gene dose-related differences in regional [^{11}C]PiB binding have been previously described (Snellman et al., 2023). Briefly, images were preprocessed using an automated pipeline (Karjalainen et al., 2020), which included co-registration to a T1-weighted MRI scan, ROI parcellation and PET kinetic modelling. Cerebellar grey matter was used as reference region. [^{11}C]PiB binding was quantified as standardized uptake value ratios (SUVr) for the following ROIs: prefrontal cortex, parietal cortex, anterior cingulum, posterior cingulum, precuneus and lateral temporal cortex. These regions were averaged to obtain a volume-weighted composite (PiB-COMP) measure.

2.7. Statistical analyses

The main statistical analyses were performed using RStudio version 2022.12.0 + 353. For all numerical variables, normality was assessed with histograms, Shapiro-Wilk and Jarque-Bera tests. DTI metrics which did not fit the normal distribution were logarithmically transformed. Homoscedasticity was verified with Levene's test.

Categorical demographic variables were compared between *APOE3/3, APOE3/4* and *APOE4/4* carriers with a χ^2 test. Numerical demographic variables were compared with an ANOVA if normally distributed and a Kruskal-Wallis test was used otherwise. Statistical significance was established at $p < 0.05$ (two-sided). If significant differences were found, a Tukey's honest significant difference (HSD) or Dunn's test were used to determine which specific groups differed significantly from each other.

FA, MD, AxD and RD at each of the ROIs were compared between *APOE3/3, APOE3/4* and *APOE4/4* carriers with a one-way ANCOVA, with the age and sex being covariates of no interest. If a significant difference was found, Tukey's HSD was used to determine the direction of differences and Cohen's d was used to assess the effect size. To test that our results were independent of i) the scanner used at the time of acquisition ii) WMHs, measured as a computed Fazekas score, and other lifestyle factors including iii) smoking, iv) diabetes and v) anti-hypertensive medications, we included these five variables as covariates in a second model.

By conducting ROI analysis, we aimed to quantify diffusion in a controlled number of regions relevant to the development of AD, based on a predefined hypothesis. Moreover, the main purpose of ASIC-E4 and CIRI-5Y cohorts was not to assess white matter microstructure, which makes this study exploratory in nature. This means it may lack sufficient statistical power to detect subtle differences, thus providing false negatives. For these reasons, following the guidelines of statistical theory (Rothman, 1990) and current research (Lyall et al., 2020; Svärd et al., 2017), uncorrected alpha < 0.05 was considered nominally significant in our regional analyses. We additionally applied the false discovery rate (FDR) correction to our findings (Benjamini and Hochberg, 1995), but results are reported without correction for multiple comparisons unless stated otherwise.

To evaluate the association of DTI measures with serum NfL concentration and global Aβ deposition estimated by PiB-COMP, mean scores of FA, MD, AxD and RD were calculated by computing the voxel-weighted average of our ROIs. Spearman's rank-order test was used to assess the correlation coefficient in the whole sample and stratified by their *APOE* status, which was considered significant at $p < 0.05$. We examined possible interactions between *APOE* genotype and DTI on serum NfL and global Aβ with multiple linear regression, where *APOE* genotype and FA, MD, AxD or RD and the interaction term were added as predictors.

Voxel-wise differences were assessed with the GLM design using the Randomise tool in FSL (Winkler et al., 2014). DTI metrics were compared between *APOE3/3*, *APOE3/4* and *APOE4/4* carriers using a one-way ANCOVA, including mean-centered age and sex as covariates of no interest. The number of permutations was set to 5000 based on the threshold-free cluster enhancement (TFCE) (Smith and Nichols, 2009). Results were considered significant at $p < 0.05$ with the family wise error (FWE) correction for multiple comparisons. Clusters were labelled according to JHU ICBM-DTI-81 white matter labels atlas.

3. Results

3.1. Study population

Table 1 shows the distribution of demographic variables stratified by *APOE* genotype. Our sample included ninety-six participants (mean age = 70.7, SD = 5.22), of whom 63% were females. All groups were well-matched for age ($p = 0.29$), sex ($p = 0.89$), educational level ($p = 0.68$) and body-mass index ($p = 0.16$). A proportion of the participants smoked (2%), had diabetes (4%) or were taking anti-hypertensive medication (50%), but there were no significant differences across groups (all $p > 0.22$). There were significant differences in [^{11}C]PiB SUVrs between *APOE3/3*, *APOE3/4* and *APOE4/4* carriers ($p = 0.0010$). *APOE3/3* showed significantly lower Aβ deposition than *APOE4/4* ($p = 0.0013$) and *APOE3/4* ($p = 0.017$).

3.2. Regional analysis

DTI variables for the *APOE3/3, APOE3/4* and *APOE4/4* groups are presented in Fig. 2A-D. First, there were no differences in FA between *APOE3/3, APOE3/4* and *APOE4/4* in any of the chosen ROIs (all $p > 0.13$, ANCOVA, Fig. 2A), whereas *APOE4/4* showed increased MD in the B-CC ($F = 3.37$, $p = 0.039$, ANCOVA) when compared to *APOE3/4* ($p = 0.0053$, Cohen's d = 0.68) and *APOE3/3* ($p = 0.026$, Cohen's d = 0.45) (Fig. 2B). In this region, *APOE4/4* also exhibited higher RD ($F = 3.40$, $p = 0.038$, ANCOVA) than *APOE3/4* ($p = 0.0049$, Cohen's d = 0.69) and *APOE3/3* ($p = 0.042$, Cohen's d = 0.39) (Fig. 2C). A significant increase in AxD was also found in the RC-CG ($F = 3.94$, $p = 0.023$, ANCOVA) when comparing *APOE4/4* against *APOE3/4* ($p = 0.012$, Cohen's d = 0.41) and *APOE3/3* ($p = 0.040$, Cohen's d = 0.39) (Fig. 2D). No significant differences in regional MD, AxD nor RD were found between *APOE3/3* and *APOE3/4*. All of the results remained significant after adjusting the analysis for the type of MRI scanner used during image acquisition (all $p < 0.040$), WMHs (all $p < 0.035$) and lifestyle factors including smoking, diabetes and anti-hypertensive medication (all $p < 0.048$). However, no significant differences remained after FDR correction (all fully adjusted $p > 0.21$).

Group comparisons including *APOE2/3* carriers ($n = 5$) are shown in Supplementary Fig. 1. *APOE2/3* carriers showed increased MD and RD when compared to *APOE3/4*. They also exhibited a higher AxD than *APOE3/4* and *APOE3/3* carriers.

Table 1
Demographic variables.

	APOE3/3	*APOE3/4*	*APOE4/4*	*p*-value[a]
n	37	39	20	
APOE4 alleles	0	1	2	
Age (years), mean (SD)	71.2 (5.62)	71.0 (5.04)	69.0 (4.72)	0.29
Sex (M/F), n (%)	15 / 22 (41% / 59%)	14 / 25 (36% / 64%)	7 / 13 (35% / 65%)	0.89
Education, n (%)				0.68
Primary school	13 (35%)	11 (28%)	6 (30%)	
Middle school	9 (24%)	10 (26%)	6 (30%)	
High school	9 (24%)	7 (18%)	6 (30%)	
College or university	6 (16%)	11 (28%)	2 (10%)	
Currently smoking, n (%)	0 (0%)	2 (5%)	0 (0%)	0.22
Diabetes, n (%)	3 (8%)	1 (3%)	0 (0%)	0.27
Anti-hypertensive medication, n (%)	21 (57%)	17 (44%)	10 (50%)	0.52
BMI (kg/m^2), mean (SD)	28.1 (5)	26.4 (3.63)	26.3 (4.17)	0.16
Scanner (scanner1 /scanner2), n (%)	25 / 12 (68% / 32%)	35 / 4 (90% / 10%)	13 / 7 (65% / 35%)	**0.033**
Fazekas score, median (IQR)	0.92 (0.00–1.46)	0.92 (0.00–1.30)	1.15 (0.18–1.71)	0.56
Serum NfL pg/ml, median (IQR)	16.6 (13.9–19.7)	19.6 (13.6–23.4)	22.0 (15.7–30.1)	0.19
[^{11}C]PiB SUVr, median (IQR)	1.54 (1.43–1.77)	1.82 (1.52–2.41)*	2.53 (1.75–2.86)**	**0.0010**

Note: [a]The p-value refers to overall difference among the groups. Categorical variables were analyzed with a χ^2 test and numerical variables were analyzed with a one-way ANOVA or Kruskal-Wallis test, pair-wise differences compared to APOE3/3 carriers are shown with star symbols: * $p < 0.05$, ** $p < 0.01$.
M = male, F = female, SUVr = standardized uptake value ratio, BMI = body mass index, H = high, L = low, scanner1 = Philips Ingenuity 3.0 T TF PET-MR, scanner2 = Philips Ingenia 3.0 T systems.

3.3. Whole-brain analysis

Results obtained from the whole-brain analysis are presented in Fig. 3. First, we did not find any significant differences between *APOE3/3, APOE3/4* and *APOE4/4* groups (all $p > 0.09$, FWE-corrected). However, an exploratory analysis with a more liberal threshold (uncorrected $p < 0.001$) revealed subtle differences in MD and AxD between *APOE3/3*, *APOE3/4* and *APOE4/4* (Supplementary Fig. 3). The remaining contrasts, corresponding to pairwise comparisons, showed that *APOE4/4* carriers exhibited a higher MD than *APOE3/4* and *APOE3/3* carriers (Fig. 3A), in line with the ROI-level findings. In addition, *APOE3/4* carriers showed a greater AxD than *APOE3/3* (Fig. 3B).

3.4. Association between DTI parameters and serum NfL concentrations

We found that, in our cognitively unimpaired sample, higher serum NfL levels were associated with higher MD ($r = 0.33$ $p = 0.0019$), RD ($r = 0.36$, $p = 0.00061$) and AxD ($r = 0.31$, $p = 0.0028$) (Fig. 4). However, no significant association was detected with FA. Interaction analyses for DTI measures and *APOE* genotype showed no interaction for 'FA × *APOE* genotype' on NfL levels ($F = 0.44$, $p = 0.65$). In contrast, significant interactions were found for 'MD × *APOE* genotype', ($F = 4.26$, $p = 0.017$) and 'RD × *APOE* genotype' ($F = 4.99$, $p = 0.0090$) on serum NfL.

When stratified by the *APOE* group, we did not find any significant correlation between DTI scalars and serum NfL levels in *APOE4* non-carriers (all $p > 0.25$). The correlation between MD and serum NfL concentrations was mostly driven by *APOE3/4* carriers ($r = 0.55$, $p = 0.00083$) and, to a lesser extent, by *APOE4/4* carriers ($r = 0.48$, $p = 0.034$). RD similarly correlated with serum NfL in *APOE3/4* carriers ($r = 0.55$, $p = 0.00085$) and *APOE4/4* carriers ($r = 0.5$, $p = 0.023$). The correlation between AxD and serum NfL levels was solely driven by *APOE3/4* carriers ($r = 0.5$, $p = 0.0026$). *APOE4/4* carriers showed a trend towards a positive correlation which did not reach significance ($r = 0.39$, $p = 0.089$).

3.5. Association between DTI parameters and brain Aβ load

High brain Aβ load was associated with a higher MD ($r = 0.29$, $p = 0.0063$), RD ($r = 0.26$, $p = 0.013$) and AxD ($r = 0.33$, $p = 0.013$) (Fig. 5). Once more, no significant correlations were found for FA. Interaction analyses for DTI measures and *APOE* genotype on Aβ load showed no interaction for 'FA × *APOE* genotype' ($F = 0.060$, $p = 0.94$). There was a significant interaction between RD and *APOE* genotype ($F = 5.11$, $p = 0.0080$), between MD and *APOE* genotype ($F = 5.48$, $p = 0.0058$) and between AxD and *APOE* genotype ($F = 5.20$, $p = 0.0075$) on Aβ deposition.

Stratification by *APOE* genotype revealed no significant correlations between DTI scalars and brain Aβ load in non-carriers (all $p > 0.18$). In the *APOE4/4* group, only AxD significantly correlated with Aβ load ($r = 0.53$, $p = 0.02$), whereas the correlation with MD was borderline significant ($r = 0.44$, $p = 0.058$). The remaining correlations were driven by *APOE3/4* carriers (all $p < 0.015$).

4. Discussion

We aimed to test the differential effects of *APOE4* hetero- and homozygosity on white matter microstructure in elderly healthy individuals ($n = 96$). In recent research, the hypothesis that *APOE4* allele affects white matter microstructure has resurfaced (Blanchard et al., 2022; Lee et al., 2022). We demonstrated that DTI scalars, including MD, RD and AxD, were higher in *APOE4/4* homozygotes when compared to *APOE3/4* and *APOE3/3* carriers, and that indicators of white matter impairment correlated with biomarkers of AD and neurodegeneration in this cognitively well-preserved population.

4.1. Main findings

We found increased MD and RD in the body of corpus callosum in *APOE4/4* carriers. *APOE4/4* also exhibited a higher AxD than *APOE3/4* and *APOE3/3* carriers in the right cingulum adjacent to the cingulate gyrus. However, we did not find any differences in FA between our three groups. These findings are in line with previous DTI studies, where no associations between *APOE4* allele and FA have been found (Dowell et al., 2013; Honea et al., 2009; Nyberg and Salami, 2014; Rieckmann et al., 2016; Westlye et al., 2012). A previous DTI study which included a small group of *APOE4/4* carriers ($n = 10$) did not report differences between *APOE4* homo- and heterozygotes (Persson et al., 2006), but we expected that subtle differences would appear if we increased the sample size. Our findings in DTI analysis indicate that *APOE4/4* carriers show local increases in diffusivity. These subjects already have high loads of Aβ in their brains (Snellman et al., 2023). Thus, these differences in white matter microstructure are unlikely to be due to age-related changes and might reflect white matter impairment.

We did not find the gene-dose effects we expected, because *APOE3/4* and *APOE3/3* carriers did not significantly differ from each other at a regional level. DTI scalars do not necessarily reflect white matter

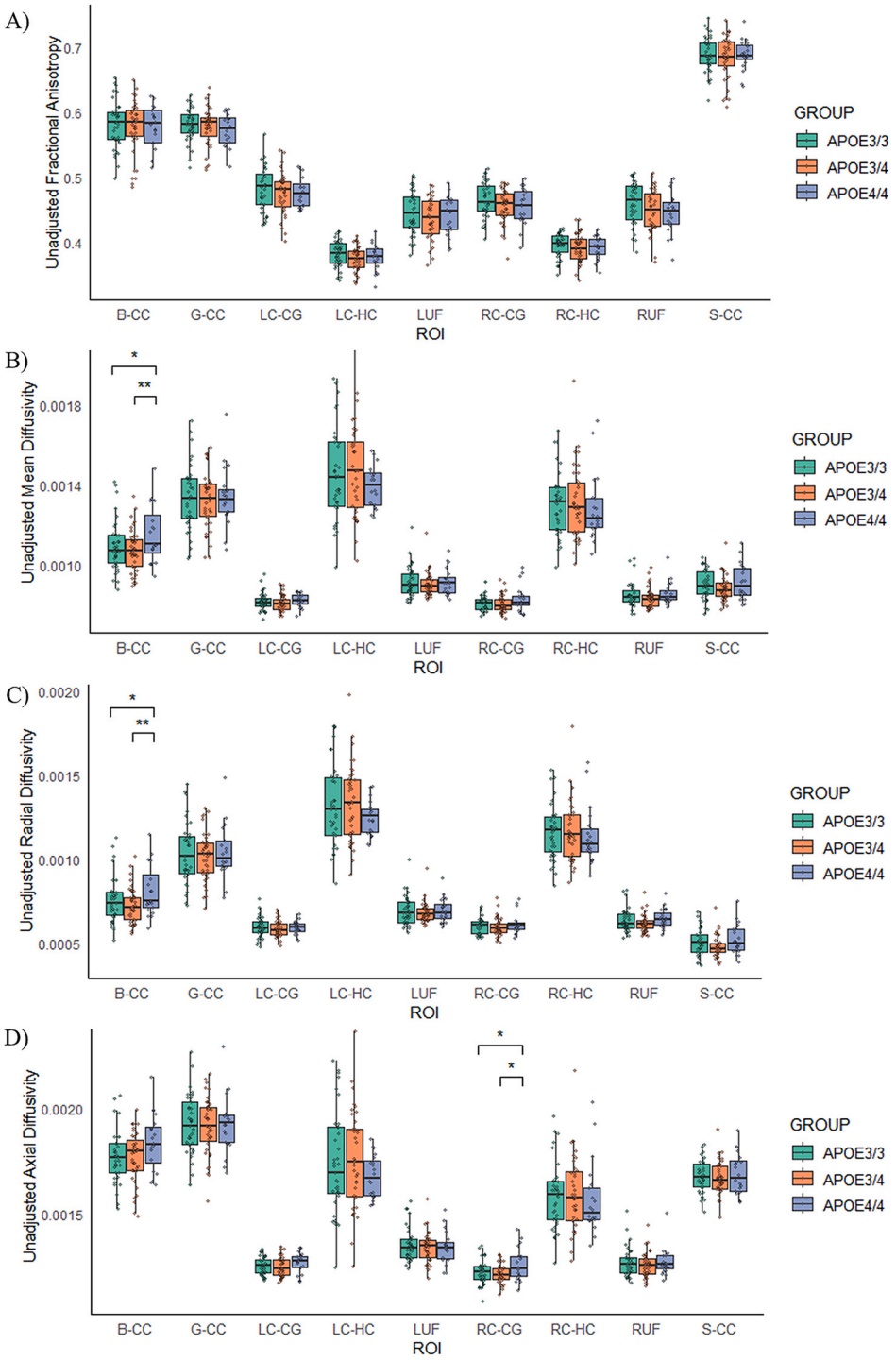

Fig. 2. Regional differences in fractional anisotropy (A), mean diffusivity (B), radial diffusivity (C) and axial diffusivity (D) between *APOE3/3*, *APOE3/4* and *APOE4/4* estimated by ANCOVA, corrected for age and sex. Pairwise differences in Tukey's HSD test are shown with star symbols: * $p < 0.05$, ** $p < 0.01$.
B-CC = body of corpus callosum, G-CC = genu of corpus callosum, LC-CG = left cingulum adjacent to cingulate gyrus, LC-HC = left cingulum adjacent to hippocampus, LUF = left uncinate fasciculus, RC-CG = right cingulum adjacent to cingulate gyrus, RC-HC = right cingulum adjacent to hippocampus, RUF = right uncinate fasciculus, S-CC = splenium of corpus callosum.

integrity (Jones et al., 2013), and tissue microstructure can be affected by conditions unrelated to AD. Furthermore, *APOE3/4* carriers who are still cognitively healthy at approximately 70 years probably have only very subtle AD-related changes in their brain.

Differences in DTI scalar measures were not significant at whole-brain level when we compared the three *APOE4* groups to each other (all FWE-corrected $p > 0.09$); however, a few small, significant clusters appeared when we used a more liberal threshold (uncorrected $p < 0.001$). *APOE4/4* carriers showed increased MD compared to *APOE3/4* and *APOE3/3*, and *APOE3/4* exhibited a higher AxD than *APOE3/3* (FWE-corrected $p < 0.05$), thus aligning to our ROI analysis. TBSS was run after our primary analysis to confirm our findings. It is possible that the whole-brain ANCOVA did not reach a significant threshold because the ROI approach focused only on regions vulnerable to AD pathology,

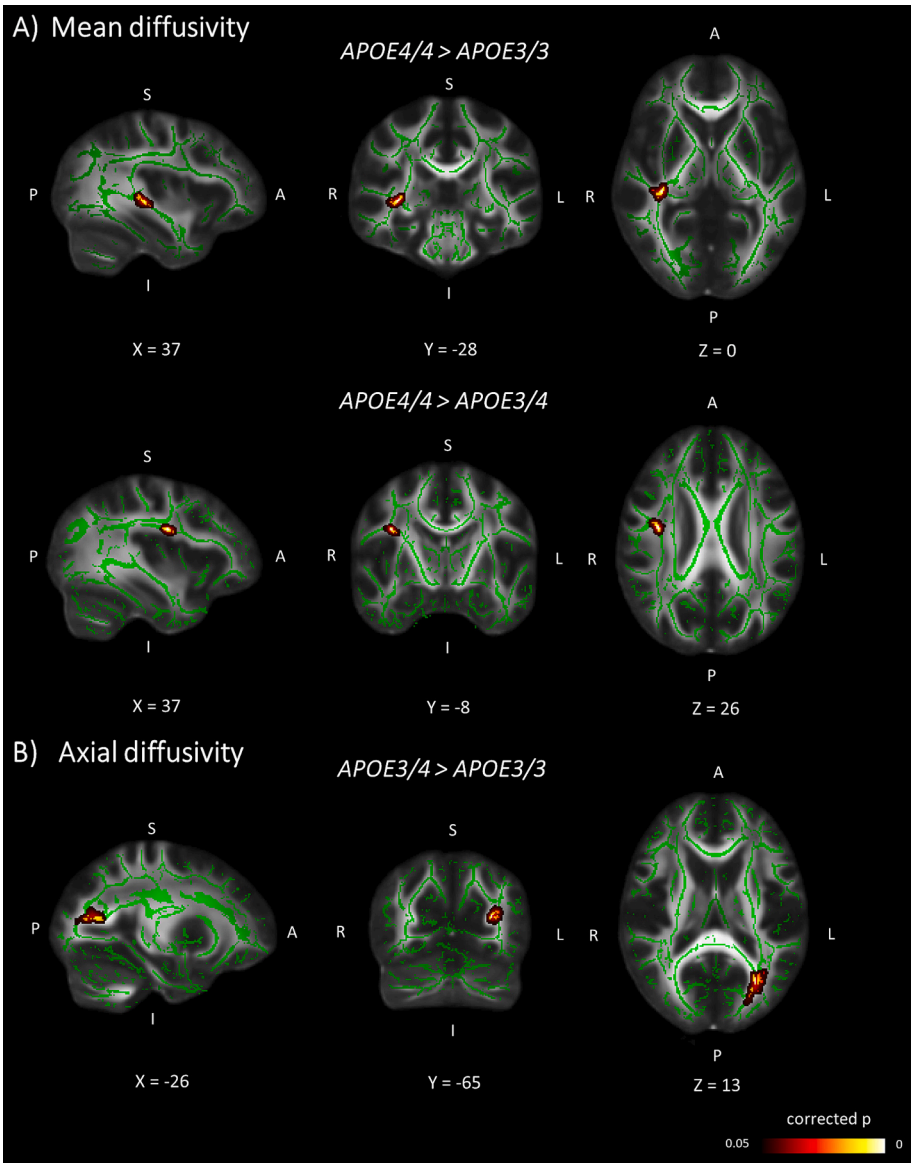

Fig. 3. Pairwise comparisons with TBSS (shown in black-red) projected over the mean FA skeleton (shown in green) and the FMRIB58_FA_1mm template at $p < 0.05$, corrected for age and sex and controlling the family wise error rate with TFCE. *APOE4/4* show a higher mean diffusivity than *APOE3/4* in the internal capsule and a higher mean diffusivity than *APOE3/3* carriers in the right superior longitudinal fasciculus (A); *APOE3/4* show a greater axial diffusivity than *APOE3/3* in a cluster comprising part of the splenium of corpus callosum, left posterior thalamic radiation and left posterior corona radiata (B). Clusters have been filled with "tbss fill" in FSL, for visualization purposes. (For interpretation of the references to colour in this figure legend, the reader is referred to the web version of this article.)

whereas analysis of large brain maps included the whole white matter skeleton.

4.2. Methodological considerations

We chose a set of ROIs (B-CC, G-CC, S-CC, LC-CG, RC-CG, LC-CH, RC-CH, RUF, LUF) aimed to specifically test the effects of early AD, since *APOE4* carriers in a subset of our cohort already exhibited abnormalities in biomarkers of AD (Snellman et al., 2023; Koivumäki et al., 2023). We found significantly increased diffusivity in the cingulum and corpus callosum of *APOE4* homozygotes. These regions connect the entorhinal cortex and the cerebral hemispheres, respectively, and they are fundamental for higher cognitive functions. Microstructural alterations in these tracts have been found in patients of AD (Esrael et al., 2021; Gallagher et al., 2023; Lim et al., 2012; Palesi et al., 2018), and already in healthy *APOE4* heterozygotes (Adluru et al., 2014; Cai et al., 2017). We explored the tissue microstructure of these ROIs under the premise that white matter impairment might precede cognitive decline (Gallagher et al., 2023). In addition, damage to the fornix has been consistently reported in patients with dementia (Aggleton et al., 2016; Oishi and Lyketsos, 2014), so we initially selected this region for our study. Despite its relevance from the biological perspective, the fornix is susceptible to PVEs, given its proximity to cerebrospinal fluid (Oishi and Lyketsos, 2014; Rieckmann et al., 2016). Although FA is quantified between 0 and 1, FA values below 0.20 are unlikely to represent white matter tracts (Rieckmann et al., 2016; Smith et al., 2006). Of our subjects, 30.7% exhibited values of FA < 0.2 in the fornix before thresholding, while FA was consistently higher in the remaining regions. Thus, the fornix was not included as ROI in our final analyses.

In our statistical analyses, we controlled for possible nuisance covariates, including age, sex, diabetes, smoking, anti-hypertensive medication, type of scanner used during acquisition and Fazekas scores. WMHs have been linked to cognitive decline and an increased risk for dementia (De Groot et al., 2001; Tubi et al., 2020). AD and the

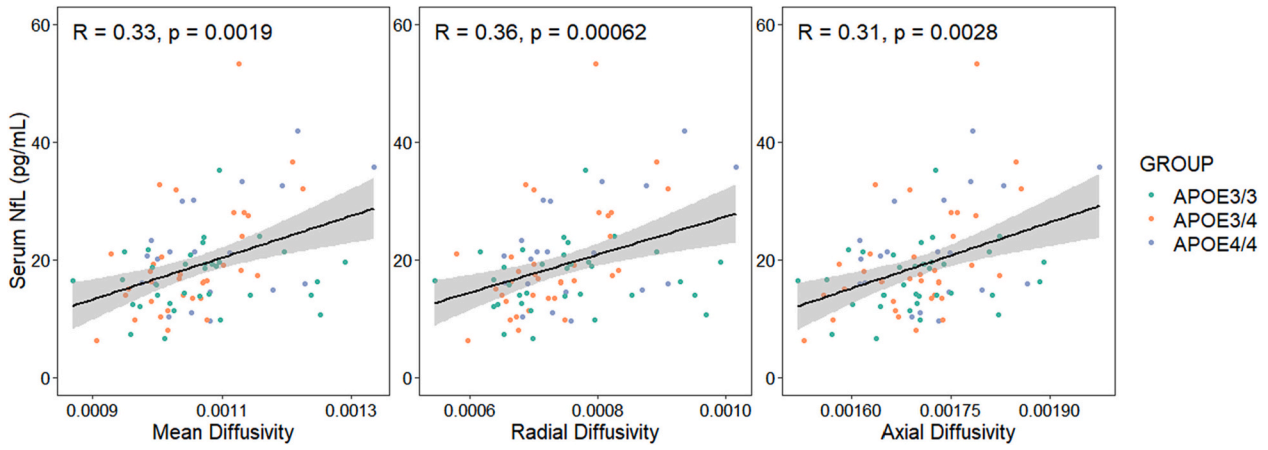

Fig. 4. Spearman's correlation coefficients between DTI metrics and serum NfL concentrations. High serum levels of NfL positively correlated with mean, radial and axial diffusivity in the whole sample, but not in subjects who did not carry any *APOE4* alleles.
NfL = neurofilament light chain.

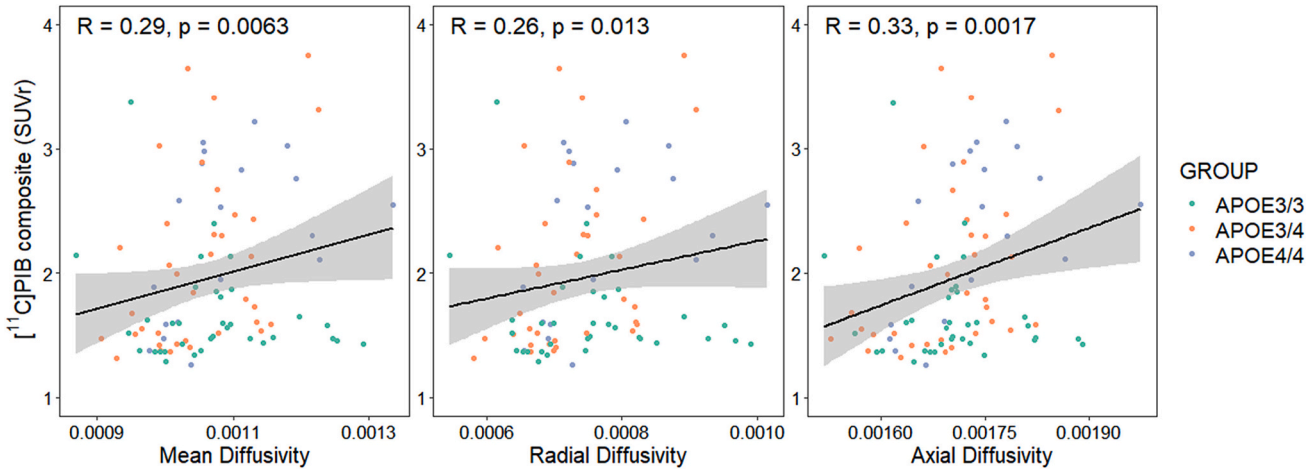

Fig. 5. Spearman's correlation coefficients between DTI metrics and Aβ deposition. High [^{11}C]PiB uptake positively correlated with mean, radial and axial diffusivity in the whole sample, but not in subjects who did not carry any *APOE4* alleles.

APOE4 allele have been previously associated with WMHs (Lyall et al., 2020; Palesi et al., 2018), although the Fazekas score did not significantly vary across *APOE* groups within our cohort. Our results remained significant when we adjusted our analyses for lifestyle factors, WMHs and type of scanner. Moreover, these variables did not improve the explanatory value of our models (adjusted R^2 increased on average 0.012), hence we decided to only include sex and age as covariates in our main results, to avoid overadjustment.

The effect sizes of our results were mostly small, but we found medium effects of *APOE4* homozygosity in the body of corpus callosum (Cohen's $d > 0.50$). The regional differences in MD, RD and AxD were attenuated when we implemented FDR correction. As it has been previously noted (Cox et al., 2016; Lyall et al., 2020; Rothman, 1990), adjusting for type-1 error when analyzing brain MRI phenotypes might be overly cautious, and it is more reliable to test the replicability of findings with different cohorts.

4.3. *APOE2* allele and white matter microstructure

The *APOE2* allele is generally considered neuroprotective (Nagy et al., 1995), but its effects on white matter microstructure have rarely been investigated, and with inconsistent results (Chiang et al., 2012; Lyall et al., 2014). We expected the *APOE2* allele to protect white matter tracts, but our exploratory supplemental findings that they show local increases in diffusivity. DTI scalar measures are affected by numerous factors. Our sample of *APOE2/3* carriers was advanced in age and they may have developed non-AD related pathologies that influenced these results. However, since our *APOE2* carrier group had only five subjects, we cannot provide conclusive insights on this topic.

4.4. DTI and other biomarkers of neurodegeneration

As our secondary objective, we aimed to expand current literature by relating our findings using DTI analysis with additional biomarkers in cognitively unimpaired at-risk individuals. We selected serum NfL as a biomarker of interest, since this biomarker reflects the intensity of axonal degeneration (Gaetani et al., 2019). Aβ load estimated by PET was chosen because *APOE4* allele induces Aβ deposition (Husain et al., 2021) that could affect white matter integrity (Rieckmann et al., 2016).

We found no correlations between FA and serum NfL levels. Increased NfL concentrations were associated with increased diffusivity scores (MD, RD and AxD) in the whole sample, but not in *APOE3/3* carriers, although these correlations were more prominent in subjects carrying only one *APOE4* allele. The associations found in the present study highlight the value of DTI and serum NfL as biomarkers for axonal degeneration, confirming their potential to detect white matter impairment in subjects at genetic risk for AD.

Aβ load directly correlated with MD, RD and AxD. *APOE3/3* and *APOE3/4* carriers in our cohort had lower Aβ load than *APOE4/4,* and they exhibited lower diffusivity. The relationship between Aβ and DTI differs across cohorts and regions (Racine et al., 2014; Wang et al., 2020), presumably due to model constraints (Douaud et al., 2011). Numerous studies have failed to link the *APOE* gene with early white matter impairment, thus supporting the idea that white matter abnormalities might be better explained by the pathology of AD than the *APOE* genotype. However, it is not possible to deduce from these findings whether Aβ affects white matter microstructure, or both increased diffusivity and Aβ load are a consequence of the pathology the brain experiences in AD.

4.5. Strengths and limitations

A major strength of this project is the recruitment of 20 healthy *APOE4/4* carriers who underwent MRI, PET and had serum samples available. Thanks to the collaboration with Auria biobank during recruitment, it was possible to include sufficient *APOE4/4* carriers to conduct a separate group analysis, therefore improving the statistical power.

This study also has several limitations. We used two scanners during image acquisition, with slightly different protocols, and uneven distributions among groups. This introduced an additional confound to our analyses, although it did not influence our results. The inability to accurately represent regions with crossing fibers is an inherent limitation of the DTI model. Brain regions including UF and C-HC, where we did not find significant group differences, show large orientation dispersion (Gallagher et al., 2023), which can indicate the presence of crossing fibers. Other limitations are related to our sample. Firstly, our study cohort did not include a sufficiently large proportion of *APOE2/3* carriers to analyze these participants as a separate group. Secondly, the age range of our healthy *APOE4/4* carriers was slightly younger when compared to the other groups. Elderly non-carriers might have developed other pathologies. The DTI findings did not correlate with AD biomarkers in the non-carrier group, which supports the theory that white matter degeneration is a sign of early AD in subjects at genetic risk for the disease, but not in non-*APOE4* carriers.

5. Conclusions

Our main finding was that healthy elderly *APOE4/4* carriers showed significantly increased MD, RD and AxD compared to *APOE3/4* and *APOE3/3* carriers in regions vulnerable to AD. These indicators positively correlated with Aβ deposition and serum NfL levels in subjects who carried one or two *APOE4* alleles. The reported effects are mild and should be verified by independent cohorts.

This study emphasizes the importance of studying the effects of *APOE4* homozygosity and heterozygosity separately, by demonstrating significant differences in white matter microstructure between these groups and their association to other biomarkers for AD.

Funding

CT received funding from the Finnish Brain Foundation, Finnish Governmental Research Funding (VTR) and the University of Turku Graduate School. LE was funded by the Paulo Foundation, the Juho Vainio Foundation and Finnish Governmental Research Funding (VTR). EP was supported by the Finnish Governmental Research Funding (VTR) for Turku University Hospital, The Yrjö Jahnsson Foundation, the Betania Foundation, the Paulo Foundation and the Uulo Arhio Memorial Foundation. HZ is a Wallenberg Scholar supported by grants from the Swedish Research Council (#2022-01018 and #2019-02397), the European Union's Horizon Europe Research and Innovation Programme under grant agreement No 101053962, Swedish State Support for Clinical Research (#ALFGBG-71320), the Alzheimer Drug Discovery Foundation (ADDF), USA (#201809-2016862), the AD Strategic Fund and the Alzheimer's Association (#ADSF-21-831376-C, #ADSF-21-831381-C, and #ADSF-21-831377-C), the Bluefield Project, the Olav Thon Foundation, the Erling-Persson Family Foundation, Stiftelsen för Gamla Tjänarinnor, Hjärnfonden, Sweden (#FO2022-0270), the European Union's Horizon 2020 Research and Innovation Programme under the Marie Skłodowska-Curie grant agreement No 860197 (MIRIADE), the European Union Joint Programme – Neurodegenerative Disease Research (JPND2021-00694), the National Institute for Health and Care Research University College London Hospitals Biomedical Research Centre, and the UK Dementia Research Institute at UCL (UKDRI-1003). KB is supported by the Swedish Research Council (#2017-00915 and #2022-00732), the Swedish Alzheimer Foundation (#AF-930351, #AF-939721 and #AF-968270), Hjärnfonden, Sweden (#FO2017-0243 and #ALZ2022-0006), the Swedish state under the agreement between the Swedish Government and the County Councils, the ALF-agreement (#ALFGBG-715986 and #ALFGBG-965240), the European Union Joint Program for Neurodegenerative Disorders (JPND2019-466-236), the Alzheimer's Association 2021 Zenith Award (ZEN-21-848495), and the Alzheimer's Association 2022–2025 Grant (SG-23-1038904 QC). JR has received grants from the Sigrid Juselius Foundation and Finnish Governmental Research Funding (VTR). AS was supported by the Emil Aaltonen foundation, the Paulo Foundation, the Orion Research Foundation sr, Finnish Governmental Research Funding (ERVA) for Turku University Hospital (#310962) and Research Council of Finland (#341059).

CRediT authorship contribution statement

Claudia Tato-Fernández: Writing – review & editing, Writing – original draft, Formal analysis. **Laura L. Ekblad:** Writing – review & editing, Supervision, Formal analysis, Conceptualization. **Elina Pietilä:** Writing – review & editing, Formal analysis. **Virva Saunavaara:** Writing – review & editing, Validation, Methodology. **Semi Helin:** Writing – review & editing, Methodology. **Riitta Parkkola:** Writing – review & editing, Validation, Methodology. **Henrik Zetterberg:** Writing – review & editing, Methodology. **Kaj Blennow:** Writing – review & editing, Methodology. **Juha O. Rinne:** Writing – review & editing, Supervision, Conceptualization. **Anniina Snellman:** Writing – review & editing, Writing – original draft, Supervision, Project administration, Funding acquisition, Formal analysis, Conceptualization.

Declaration of competing interest

HZ has served at scientific advisory boards and/or as a consultant for Abbvie, Acumen, Alector, Alzinova, ALZPath, Annexon, Apellis, Artery Therapeutics, AZTherapies, Cognito Therapeutics, CogRx, Denali, Eisai, Merry Life, Nervgen, Novo Nordisk, Optoceutics, Passage Bio, Pinteon Therapeutics, Prothena, Red Abbey Labs, reMYND, Roche, Samumed, Siemens Healthineers, Triplet Therapeutics, and Wave, has given lectures in symposia sponsored by Alzecure, Biogen, Cellectricon, Fujirebio, Lilly, and Roche, and is a co-founder of Brain Biomarker Solutions in Gothenburg AB (BBS), which is a part of the GU Ventures Incubator Program (not within the scope of the submitted work).

KB has served as a consultant and on advisory boards for Acumen, ALZPath, BioArctic, Biogen, Eisai, Lilly, Moleac Pte. Ltd., Novartis, Ono Pharma, Prothena, Roche Diagnostics, and Siemens Healthineers; has served at data monitoring committees for Julius Clinical and Novartis; has given lectures, produced educational materials and participated in educational programs for AC Immune, Biogen, Celdara Medical, Eisai and Roche Diagnostics; and is a co-founder of Brain Biomarker Solutions in Gothenburg AB (BBS), which is a part of the GU Ventures Incubator Program, not related to the work presented in this paper.

Data availability

Data will be made available on request.

Acknowledgments

The authors would like to acknowledge the study participants for their altruistic contribution and the personal at Turku PET Centre for collecting the data for this study.

Appendix A. Supplementary data

Supplementary data to this article can be found online at https://doi.org/10.1016/j.nbd.2024.106439.

References

Adluru, N., Destiche, D.J., Lu, S.Y.F., Doran, S.T., Birdsill, A.C., Melah, K.E., Okonkwo, O. C., Alexander, A.L., Dowling, N.M., Johnson, S.C., Sager, M.A., Bendlin, B.B., 2014. White matter microstructure in late middle-age: effects of apolipoprotein E4 and parental family history of Alzheimer's disease. NeuroImage Clin. 4, 730–742. https://doi.org/10.1016/j.nicl.2014.04.008.

Aggleton, J.P., Pralus, A., Nelson, A.J.D., Hornberger, M., 2016. Thalamic pathology and memory loss in early Alzheimer's disease: moving the focus from the medial temporal lobe to Papez circuit. Brain 139 (7), 1877–1890. https://doi.org/10.1093/brain/aww083.

Alexander, A.L., Eun Lee, J., Lazar, M., Field, A.S., 2007. Diffusion tensor imaging of the brain. Neurotherapeutics 4, 316–329. https://doi.org/10.1016/j.nurt.2007.05.011.

Andersson, J.L.R., Sotiropoulos, S.N., 2016. An integrated approach to correction for off-resonance effects and subject movement in diffusion MR imaging. NeuroImage 125, 1063–1078. https://doi.org/10.1016/j.neuroimage.2015.10.019.

Andersson, J.L.R., Skare, S., Ashburner, J., 2003. How to correct susceptibility distortions in spin-echo echo-planar images: application to diffusion tensor imaging. NeuroImage 20 (2), 870–888. https://doi.org/10.1016/S1053-8119(03)00336-7.

Andersson, J.L.R., Graham, M.S., Zsoldos, E., Sotiropoulos, S.N., 2016. Incorporating outlier detection and replacement into a non-parametric framework for movement and distortion correction of diffusion MR images. NeuroImage 141, 556–572. https://doi.org/10.1016/j.neuroimage.2016.06.058.

Bachman, A.H., Lee, S.H., Sidtis, J.J., Ardekani, B.A., 2014. Corpus callosum shape and size changes in early Alzheimer's disease: A longitudinal MRI study using the oasis brain database. J. Alzheimers Dis. 39 (1), 71–78. https://doi.org/10.3233/JAD-131526.

Bagepally, B.S., Halahalli, H.N., John, J.P., Kota, L., Purushottam, M., Mukherjee, O., Sivakumar, P.T., Bharath, S., Jain, S., Varghese, M., 2012. Apolipoprotein E4 and brain white matter integrity in Alzheimer's disease: tract-based spatial statistics study under 3-tesla MRI. Neurodegener. Dis. 10 (1–4), 145–148. https://doi.org/10.1159/000334761.

Bartzokis, G., 2011. Alzheimer's disease as homeostatic responses to age-related myelin breakdown. Neurobiol. Aging 32 (8), 1341–1371. https://doi.org/10.1016/j.neurobiolaging.2009.08.007.

Basser, P.J., Pierpaoli, C., 1996. Microstructural and physiological features of tissues elucidated by quantitative-diffusion-tensor MRI. J. Magn. Reson. B 111 (3), 209–219. https://doi.org/10.1006/jmrb.1996.0086.

Basser, P.J., Mattiello, J., Lebihan, D., 1994. Estimation of the effective self-diffusion tensor from the NMR spin Echo. J. Magn. Reson. B 103 (3), 247–254. https://doi.org/10.1006/JMRB.1994.1037.

Benjamini, Y., Hochberg, Y., 1995. Controlling the false discovery rate: A practical and powerful approach to multiple testing. J. R. Stat. Soc. B. Methodol. 57 (1), 289–300. https://doi.org/10.1111/J.2517-6161.1995.TB02031.X.

Blanchard, J.W., Akay, L.A., Davila-Velderrain, J., von Maydell, D., Mathys, H., Davidson, S.M., Effenberger, A., Chen, C.-Y., Maner-Smith, K., Hajjar, I., Ortlund, E. A., Bula, M., Agbas, E., Ng, A., Jiang, X., Kahn, M., Blanco-Duque, C., Lavoie, N., Liu, L., Tsai, L.-H., 2022. APOE4 impairs myelination via cholesterol dysregulation in oligodendrocytes. Nature 611, 769–779. https://doi.org/10.1038/s41586-022-05439-w.

Bronge, L., Bogdanovic, N., Wahlund, L.-O., 2002. Postmortem MRI and histopathology of white matter changes in Alzheimer brains. Dement. Geriatr. Cogn. Disord. 13 (4), 205–212. https://doi.org/10.1159/000057698.

Cai, S., Jiang, Y., Wang, Y., Wu, X., Ren, J., Lee, M.S., Lee, S., Huang, L., 2017. Modulation on brain gray matter activity and white matter integrity by APOE ε4 risk gene in cognitively intact elderly: A multimodal neuroimaging study. Behav. Brain Res. 322, 100–109. https://doi.org/10.1016/j.bbr.2017.01.027.

Cavedo, E., Lista, S., Rojkova, K., Chiesa, P.A., Houot, M., Brueggen, K., Blautzik, J., Bokde, A.L.W., Dubois, B., Barkhof, F., Pouwels, P.J.W., Teipel, S., Hampel, H., 2017. Disrupted white matter structural networks in healthy older adult APOE ε4 carriers – an international multicenter DTI study. Neuroscience 357, 119–133. https://doi.org/10.1016/j.neuroscience.2017.05.048.

Chandler, M.J., Lacritz, L.H., Hynan, L.S., Barnard, H.D., Allen, G., Deschner, M., Weiner, M.F., Cullum, C.M., 2005. A total score for the CERAD neuropsychological battery. Neurology 65 (1), 102–106. https://doi.org/10.1212/01.wnl.0000167607.63000.38.

Chiang, G.C., Zhan, W., Schuff, N., Weiner, M.W., 2012. White matter alterations in cognitively normal apoE ε2 carriers: insight into Alzheimer resistance? Am. J. Neuroradiol. 33 (7), 1392–1397. https://doi.org/10.3174/ajnr.A2984.

Corder, E.H., Saunders, A.M., Strittmatter, W.J., Schmechel, D.E., Gaskell, P.C., Small, G. W., Roses, A.D., Haines, J.L., Pericak-Vance, M.A., 1993. Gene dose of apolipoprotein E type 4 allele and the risk of Alzheimer's disease in late onset families. Science 261 (5123), 921–923. https://doi.org/10.1126/science.8346443.

Cox, S.R., Ritchie, S.J., Tucker-Drob, E.M., Liewald, D.C., Hagenaars, S.P., Davies, G., Wardlaw, J.M., Gale, C.R., Bastin, M.E., Deary, I.J., 2016. Ageing and brain white matter structure in 3,513 UK biobank participants. Nat. Commun. 7 (1), 13629. https://doi.org/10.1038/ncomms13629.

De Groot, J.C., De Leeuw, F.-E., Oudkerk, M., Hofman, A., Jolles, J., Breteler, M.M.B., 2001. Cerebral white matter lesions and subjective cognitive dysfunction the Rotterdam scan study. Neurology 56 (11), 1539–1545. https://doi.org/10.1212/wnl.56.11.1539.

Douaud, G., Jbabdi, S., Behrens, T.E.J., Menke, R.A., Gass, A., Monsch, A.U., Rao, A., Whitcher, B., Kindlmann, G., Matthews, P.M., Smith, S., 2011. DTI measures in crossing-fibre areas: increased diffusion anisotropy reveals early white matter alteration in MCI and mild Alzheimer's disease. NeuroImage 55 (3), 880–890. https://doi.org/10.1016/j.neuroimage.2010.12.008.

Dowell, N.G., Ruest, T., Evans, S.L., King, S.L., Tabet, N., Tofts, P.S., Rusted, J.M., 2013. MRI of carriers of the apolipoprotein E e4 allele-evidence for structural differences in normal-appearing brain tissue in e4+ relative to e4- young adults. NMR Biomed. 26 (6), 674–682. https://doi.org/10.1002/nbm.2912.

Ekblad, L.L., Johansson, J., Helin, S., Viitanen, M., Laine, H., Puukka, P., Jula, A., Rinne, J.O., 2018. Midlife insulin resistance, APOE genotype, and late-life brain amyloid accumulation. Neurology 90 (13), 1150–1157. https://doi.org/10.1212/WNL.0000000000005214.

Espeseth, T., Westlye, L.T., Walhovd, K.B., Fjell, A.M., Endestad, T., Rootwelt, H., Reinvang, I., 2012. Apolipoprotein E ε4-related thickening of the cerebral cortex modulates selective attention. Neurobiol. Aging 33 (2), 304–322.e1. https://doi.org/10.1016/j.neurobiolaging.2009.12.027.

Esrael, S.M.A.M., Hamed, A.M.M., Khedr, E.M., Soliman, R.K., 2021. Application of diffusion tensor imaging in Alzheimer's disease: quantification of white matter microstructural changes. Egypt J. Radiol. Nucl. Med. 52 (1) https://doi.org/10.1186/s43055-021-00460-x.

Gaetani, L., Blennow, K., Calabresi, P., Di Filippo, M., Parnetti, L., Zetterberg, H., 2019. Neurofilament light chain as a biomarker in neurological disorders. J. Neurol. Neurosurg. Psychiatry 90 (8), 870–881. https://doi.org/10.1136/jnnp-2018-320106.

Gallagher, R.L., Koscik, R.L., Moody, J.F., Vogt, N.M., Adluru, N., Kecskemeti, S.R., Van Hulle, C.A., Chin, N.A., Asthana, S., Kollmorgen, G., Suridjan, I., Carlsson, C.M., Johnson, S.C., Dean, D.C., Zetterberg, H., Blennow, K., Alexander, A.L., Bendlin, B. B., 2023. Neuroimaging of tissue microstructure as a marker of neurodegeneration in the AT(N) framework: defining abnormal neurodegeneration and improving prediction of clinical status. Alzheimers Res. Ther. 15 (1), 180. https://doi.org/10.1186/s13195-023-01281-y.

Gharbi-Meliani, A., Dugravot, A., Sabia, S., Regy, M., Fayosse, A., Schnitzler, A., Kivimäki, M., Singh-Manoux, A., Dumurgier, J., 2021. The association of APOE ε4 with cognitive function over the adult life course and incidence of dementia: 20 years follow-up of the Whitehall II study. Alzheimers Res. Ther. 13 (1), 5. https://doi.org/10.1186/s13195-020-00740-0.

Gold, B.T., Powell, D.K., Andersen, A.H., Smith, C.D., 2010. Alterations in multiple measures of white matter integrity in normal women at high risk for Alzheimer's disease. NeuroImage 52 (4), 1487–1494. https://doi.org/10.1016/j.neuroimage.2010.05.036.

Heise, V., Filippini, N., Trachtenberg, A.J., Suri, S., Ebmeier, K.P., Mackay, C.E., 2014. Apolipoprotein E genotype, gender and age modulate connectivity of the hippocampus in healthy adults. NeuroImage 98, 23–30. https://doi.org/10.1016/j.neuroimage.2014.04.081.

Honea, R.A., Vidoni, E., Harsha, A., Burns, J.M., 2009. Impact of APOE on the healthy aging brain: A voxel-based MRI and DTI study. J. Alzheimers Dis. 18 (3), 553–564. https://doi.org/10.3233/JAD-2009-1163.

Husain, M.A., Laurent, B., Plourde, M., 2021. APOE and Alzheimer's disease: from lipid transport to physiopathology and therapeutics. Front. Neurosci. 15 https://doi.org/10.3389/fnins.2021.630502.

Ingelsson, M., Fukumoto, H., Newell, K., Growdon, J., Hedley-Whyte, E., Frosch, M., Albert, M., Hyman, B., Irizarry, M., 2004. Early Abeta accumulation and progressive synaptic loss, gliosis, and tangle formation in AD brain. Neurology 62 (6), 925–931. https://doi.org/10.1212/01.wnl.0000115115.98960.37.

Jänis, M.T., Siggins, S., Tahvanainen, E., Vikstedt, R., Silander, K., Metso, J., Aromaa, A., Taskinen, M.-R., Olkkonen, V.M., Jauhiainen, M., Ehnholm, C., 2004. Active and low-active forms of serum phospholipid transfer protein in a normal Finnish population sample. J. Lipid Res. 45 (12), 2303–2309. https://doi.org/10.1194/jlr.M400250-JLR200.

Jones, D.K., Knösche, T.R., Turner, R., 2013. White matter integrity, fiber count, and other fallacies: the do's and don'ts of diffusion MRI. NeuroImage 73, 239–254. https://doi.org/10.1016/j.neuroimage.2012.06.081.

Karjalainen, T., Tuisku, J., Santavirta, S., Kantonen, T., Bucci, M., Tuominen, L., Hirvonen, J., Hietala, J., Rinne, J.O., Nummenmaa, L., 2020. Magia: robust automated image processing and kinetic modeling toolbox for PET Neuroinformatics. Front. Neuroinform. 14 https://doi.org/10.3389/fninf.2020.00003.

Koikkalainen, J., Rhodius-Meester, H., Tolonen, A., Barkhof, F., Tijms, B., Lemstra, A.W., Tong, T., Guerrero, R., Schuh, A., Ledig, C., Rueckert, D., Soininen, H., Remes, A.M., Waldemar, G., Hasselbalch, S., Mecocci, P., Van Der Flier, W., Lötjönen, J., 2016.

Differential diagnosis of neurodegenerative diseases using structural MRI data. NeuroImage Clin. 11, 435–449. https://doi.org/10.1016/j.nicl.2016.02.019.
Koivumäki, M., Ekblad, L., Lantero-Rodriguez, J., Ashton, N., Karikari, T., Helin, S., Zetterberg, H., Blennow, K., Rinne, J., Snellman, A., 2023. Blood biomarkers of neurodegeneration associate differently with amyloid deposition, medial temporal atrophy, and cerebrovascular changes in APOE ε4-enriched cognitively unimpaired elderly. Preprint. Res. Square. https://doi.org/10.21203/rs.3.rs-3124100/v1.
Lee, Y.M., Ha, J.K., Park, J.M., Lee, B.D., Moon, E., Chung, Y.I., Kim, J.H., Kim, H.J., Mun, C.W., Kim, T.H., Kim, Y.H., 2016. Impact of apolipoprotein E4 polymorphism on the gray matter volume and the white matter integrity in subjective memory impairment without white matter Hyperintensities: voxel-based morphometry and tract-based spatial statistics study under 3-tesla MRI. J. Neuroimaging 26 (1), 144–149. https://doi.org/10.1111/jon.12207.
Lee, Y.-B., Kim, M.Y., Han, K., Kim, B., Park, J., Kim, G., Hur, K.Y., Kim, J.H., Jin, S.-M., 2022. Association between cholesterol levels and dementia risk according to the presence of diabetes and statin use: a nationwide cohort study. Sci. Rep. 12 (19383) https://doi.org/10.1038/s41598-022-24153-1.
Lesser, G.T., Beeri, M.S., Schmeidler, J., Purohit, D.P., Haroutunian, V., 2011. Cholesterol and LDL relate to Neuritic plaques and to APOE4 presence but not to neurofibrillary tangles. Curr. Alzheimer Res. 8 (3), 303–312. https://doi.org/10.2174/156720511795563755.
Li, X., Morgan, P.S., Ashburner, J., Smith, J., Rorden, C., 2016. The first step for neuroimaging data analysis: DICOM to NIfTI conversion. J. Neurosci. Methods 264, 47–56. https://doi.org/10.1016/j.jneumeth.2016.03.001.
Lim, H.K., Kim, S.J., Choi, C.G., Lee, J.-H., Kim, S.Y., Kim, H.J., Kim, N., Jahng, G.-H., 2012. Evaluation of white matter abnormality in mild Alzheimer disease and mild cognitive impairment using diffusion tensor imaging: A comparison of tract-based spatial statistics with voxel-based morphometry. Korean Soc. Magnet. Reson. Med. 16 (2), 115–123. https://doi.org/10.13104/jksmrm.2012.16.2.115.
Lyall, D.M., Harris, S.E., Bastin, M.E., Muñoz Maniega, S., Murray, C., Lutz, M.W., Saunders, A.M., Roses, A.D., del Valdés Hernández, M.C., Royle, N.A., Starr, J.M., Porteous, D.J., Wardlaw, J.M., Deary, I.J., 2014. Alzheimer's disease susceptibility genes APOE and TOMM40, and brain white matter integrity in the Lothian birth cohort 1936. Neurobiol. Aging 35 (6), 1513.e25–1513.e33. https://doi.org/10.1016/j.neurobiolaging.2014.01.006.
Lyall, D.M., Cox, S.R., Lyall, L.M., Celis-Morales, C., Cullen, B., Mackay, D.F., Ward, J., Strawbridge, R.J., McIntosh, A.M., Sattar, N., Smith, D.J., Cavanagh, J., Deary, I.J., Pell, J.P., 2020. Association between APOE e4 and white matter hyperintensity volume, but not total brain volume or white matter integrity. Brain Imag. Behav. 14 (5), 1468–1476. https://doi.org/10.1007/s11682-019-00069-9.
Mori, S., Oishi, K., Jiang, H., Jiang, L., Li, X., Akhter, K., Hua, K., Faria, A., Mahmood, A., Woods, R., Toga, A.W., Pike, G.B., Neto, P.R., Evans, A., Zhang, J., Huang, H., Miller, M.I., van Zijl, P., Mazziotta, J., 2008. Stereotaxic white matter atlas based on diffusion tensor imaging in an ICBM template. NeuroImage 40 (2), 570–582. https://doi.org/10.1016/J.NEUROIMAGE.2007.12.035.
Nagy, Z.S., Esiri, M.M., Jobst, K.A., Johnston, C., Litchfield, S., Sim, E., Smith, A.D., 1995. Influence of the apolipoprotein E genotype on amyloid deposition and neurofibrillary tangle formation in Alzheimer's disease. Neuroscience 69 (3), 757–761. https://doi.org/10.1016/0306-4522(95)00331-C.
Nierenberg, J., Pomara, N., Hoptman, M.J., Sidtis, J.J., Ardekani, B.A., Lim, K.O., 2005. Abnormal white matter integrity in healthy apolipoprotein E epsilon4 carriers. Neuroreport 16 (12), 1369–1372. https://doi.org/10.1097/01.wnr.0000174058.49521.16.
Nyberg, L., Salami, A., 2014. The APOE ε4 allele in relation to brain white-matter microstructure in adulthood and aging. Scand. J. Psychol. 55 (3), 263–267. https://doi.org/10.1111/sjop.12099.
O'Donnell, L.J., Westin, C.F., 2011. An introduction to diffusion tensor image analysis. Neurosurg. Clin. N. Am. 22 (2), 185–196. https://doi.org/10.1016/j.nec.2010.12.004.
O'Dwyer, L., Lamberton, F., Matura, S., Scheibe, M., Miller, J., Rujescu, D., Prvulovic, D., Hampel, H., 2012. White matter differences between healthy young ApoE4 carriers and non-carriers identified with tractography and support vector machines. PLoS One 7 (4). https://doi.org/10.1371/journal.pone.0036024.
Oishi, K., Lyketsos, C.G., 2014. Alzheimer's disease and the fornix. Front. Aging Neurosci. 6 (SEP) https://doi.org/10.3389/fnagi.2014.00241.
Palesi, F., De Rinaldis, A., Vitali, P., Castellazzi, G., Casiraghi, L., Germani, G., Bernini, S., Anzalone, N., Ramusino, M.C., Denaro, F.M., Sinforiani, E., Costa, A., Magenes, G., D'Angelo, E., Wheeler-Kingshott, C.A.M.G., Micieli, G., 2018. Specific patterns of white matter alterations help distinguishing Alzheimer's and vascular dementia. Front. Neurosci. 12 https://doi.org/10.3389/fnins.2018.00274.
Persson, J., Lind, J., Larsson, A., Ingvar, M., Cruts, M., Van Broeckhoven, C., Adolfsson, R., Nilsson, L.G., Nyberg, L., 2006. Altered brain white matter integrity in healthy carriers of the APOE epsilon4 allele: a risk for AD? Neurology 66 (7), 1029–1033. https://doi.org/10.1212/01.wnl.0000204180.25361.48.
Racine, A.M., Adluru, N., Alexander, A.L., Christian, B.T., Okonkwo, O.C., Oh, J., Cleary, C.A., Birdsill, A., Hillmer, A.T., Murali, D., Barnhart, T.E., Gallagher, C.L., Carlsson, C.M., Rowley, H.A., Dowling, N.M., Asthana, S., Sager, M.A., Bendlin, B.B., Johnson, S.C., 2014. Associations between white matter microstructure and amyloid burden in preclinical Alzheimer's disease: A multimodal imaging investigation. NeuroImage Clin. 4, 604–614. https://doi.org/10.1016/j.nicl.2014.02.001.
Rieckmann, A., Van Dijk, K.R.A., Sperling, R.A., Johnson, K.A., Buckner, R.L., Hedden, T., 2016. Accelerated decline in white matter integrity in clinically normal individuals at risk for Alzheimer's disease. Neurobiol. Aging 42, 177–188. https://doi.org/10.1016/j.neurobiolaging.2016.03.016.
Rothman, K., 1990. No adjustments are needed for multiple comparisons. Epidemiology 1 (1), 43–46. http://www.jstor.org/stable/20065622.
Saraste, M., Bezukladova, S., Matilainen, M., Tuisku, J., Rissanen, E., Sucksdorff, M., Laaksonen, S., Vuorimaa, A., Kuhle, J., Leppert, D., Airas, L., 2021. High serum neurofilament associates with diffuse white matter damage in MS. Neurol. Neuroimmunol. Neuroinflam. 8 (1) https://doi.org/10.1212/NXI.0000000000000926.
Schultz, S.A., Strain, J.F., Adedokun, A., Wang, Q., Preische, O., Kuhle, J., Flores, S., Keefe, S., Dincer, A., Ances, B.M., Berman, S.B., Brickman, A.M., Cash, D.M., Chhatwal, J., Cruchaga, C., Ewers, M., Fox, N.N., Ghetti, B., Goate, A., Gordon, B.A., 2020. Serum neurofilament light chain levels are associated with white matter integrity in autosomal dominant Alzheimer's disease. Neurobiol. Dis. 142 https://doi.org/10.1016/j.nbd.2020.104960.
Smith, S.M., 2002. Fast robust automated brain extraction. Hum. Brain Mapp. 17 (3), 143–155. https://doi.org/10.1002/hbm.10062.
Smith, S., Nichols, T., 2009. Threshold-free cluster enhancement: addressing problems of smoothing, threshold dependence and localisation in cluster inference. NeuroImage 44 (1), 83–98. https://doi.org/10.1016/j.neuroimage.2008.03.061.
Smith, S.M., Jenkinson, M., Woolrich, M.W., Beckmann, C.F., Behrens, T.E.J., Johansen-Berg, H., Bannister, P.R., De Luca, M., Drobnjak, I., Flitney, D.E., Niazy, R.K., Saunders, J., Vickers, J., Zhang, Y., De Stefano, N., Brady, J.M., Matthews, P.M., 2004. Advances in functional and structural MR image analysis and implementation as FSL. NeuroImage 23 (Suppl. 1). https://doi.org/10.1016/j.neuroimage.2004.07.051.
Smith, S.M., Jenkinson, M., Johansen-Berg, H., Rueckert, D., Nichols, T.E., Mackay, C.E., Watkins, K.E., Ciccarelli, O., Cader, M.Z., Matthews, P.M., Behrens, T.E.J., 2006. Tract-based spatial statistics: Voxelwise analysis of multi-subject diffusion data. NeuroImage 31 (4), 1487–1505. https://doi.org/10.1016/J.NEUROIMAGE.2006.02.024.
Snellman, A., Ekblad, L.L., Koivumäki, M., Lindgrén, N., Tuisku, J., Perälä, M., Kallio, L., Lehtonen, R., Saunavaara, V., Saunavaara, J., Oikonen, V., Aarnio, R., Löyttyniemi, E., Parkkola, R., Karrasch, M., Zetterberg, H., Blennow, K., Rinne, J.O., 2022. ASIC-E4: interplay of Beta-amyloid, synaptic density and Neuroinflammation in cognitively Normal volunteers with three levels of genetic risk for late-onset Alzheimer's disease – study protocol and baseline characteristics. Front. Neurol. 13 https://doi.org/10.3389/fneur.2022.826423.
Snellman, A., Ekblad, L.L., Tuisku, J., Koivumäki, M., Ashton, N.J., Lantero-Rodriguez, J., Karikari, T.K., Helin, S., Bucci, M., Löyttyniemi, E., Parkkola, R., Karrasch, M., Schöll, M., Zetterberg, H., Blennow, K., Rinne, J.O., 2023. APOE ε4 gene dose effect on imaging and blood biomarkers of neuroinflammation and beta-amyloid in cognitively unimpaired elderly. Alzheimers Res. Ther. 15 (1), 71. https://doi.org/10.1186/s13195-023-01209-6.
Svärd, D., Nilsson, M., Lampinen, B., Lätt, J., Sundgren, P.C., Stomrud, E., Minthon, L., Hansson, O., Van Westen, D., 2017. The effect of white matter hyperintensities on statistical analysis of diffusion tensor imaging in cognitively healthy elderly and prodromal Alzheimer's disease. PLoS One 12 (9). https://doi.org/10.1371/journal.pone.0185239.
Tubi, M.A., Feingold, F.W., Kothapalli, D., Hare, E.T., King, K.S., Thompson, P.M., Braskie, M.N., 2020. White matter hyperintensities and their relationship to cognition: effects of segmentation algorithm. NeuroImage 206. https://doi.org/10.1016/J.NEUROIMAGE.2019.116327.
Wang, Y.-J., Hu, H., Yang, Y.-X., Zuo, C.-T., Tan, L., Yu, J.-T., 2020. Regional amyloid accumulation and white matter integrity in cognitively Normal individuals. J. Alzheimers Dis. 74 (4), 1261–1270. https://doi.org/10.3233/JAD-191350.
Westlye, E.T., Hodneland, E., Haász, J., Espeseth, T., Lundervold, A., Lundervold, A.J., 2012. Episodic memory of APOE ε4 carriers is correlated with fractional anisotropy, but not cortical thickness, in the medial temporal lobe. NeuroImage 63 (1), 507–516. https://doi.org/10.1016/j.neuroimage.2012.06.072.
Winkler, A.M., Ridgway, G.R., Webster, M.A., Smith, S.M., Nichols, T.E., 2014. Permutation inference for the general linear model. NeuroImage 92, 381–397. https://doi.org/10.1016/j.neuroimage.2014.01.060.